Applied Catalysis B: Environmental 92 (2009) 462–467

Contents lists available at ScienceDirect

Applied Catalysis B: Environmental

journal homepage: www.elsevier.com/locate/apcatb

Adsorption and oxidation of NH_3 over V_2O_5/AC surface

Dekui Sun [a,b], Qingya Liu [c], Zhenyu Liu [a,c,*], Guoqing Gui [a], Zhanggen Huang [a]

[a] State Key Laboratory of Coal Conversion, Institute of Coal Chemistry, Chinese Academy of Sciences, Taiyuan 030001, PR China
[b] Graduate University of Chinese Academy of Sciences, Beijing 100039, PR China
[c] State Key Laboratory of Chemical Resource Engineering, Beijing University of Chemical Technology, Beijing 100029, PR China

ARTICLE INFO

Article history:
Received 18 May 2009
Received in revised form 24 August 2009
Accepted 5 September 2009
Available online 12 September 2009

Keywords:
V_2O_5/AC
SCR reaction
NH_3 adsorption
Oxidation
NO

ABSTRACT

V_2O_5/AC has been reported to be active for selective catalytic reduction (SCR) of NO with NH_3 at around 200 °C and resistant to SO_2 deactivation. To elucidate its SCR mechanism, adsorption and oxidation of NH_3 over V_2O_5/AC are studied in this paper using TG, MS and DRIFTS techniques. It is found that the adsorption and oxidation of NH_3 take place mainly at V=O bond of V_2O_5. A higher V_2O_5 loading results in more NH_3 adsorption on the catalyst. V_2O_5 contains both Brϕnsted and Lewis acid sites; NH_4^+ on Brϕnsted acid sites is less stable and easier to be oxidized than NH_3 on Lewis acid sites. Gaseous O_2 promotes interaction of NH_3 with AC and oxidation of NH_3 over V_2O_5/AC. NH_3 is oxidized into NH_2 and acylamide structures and then to isocyanate species, which is an intermediate for N_2 formation.

1. Introduction

Nitrogen oxides (NO_x) are major air pollutants. Selective catalytic reduction (SCR) of NO_x with NH_3 has been widely practiced in large scales to abate NO_x from flue gas [1,2], and the main catalysts have been those containing V_2O_5/TiO_2 as well as WO_3 or MoO_3 [3,4]. These catalysts are operated usually at temperatures higher than 350 °C to avoid deactivation by SO_2 at lower temperatures [2,5]. This temperature requirement demands the SCR unit to be installed at the upstream of dust removal units, which makes it difficult to retrofit existing boiler systems. In addition, mechanical strength of the catalysts has to be high to endure dust erosion. For those reasons, development of low temperature SCR catalysts, which are resistant to SO_2 deactivation and can be used at the downstream of dust removal units, has been a subject of many researches [6].

Literature has reported many low temperature SCR catalysts especially those based on carbon materials, such as activated carbon (AC) [7], carbon fibers [8–10] and AC loaded with MnO_x, FeO_x, CuO or V_2O_5 [11–16]. Among these catalysts, AC supported V_2O_5 (V_2O_5/AC) seems more promising due to its high SCR activity at 180–250 °C and resistance to SO_2 deactivation [15–19]. More importantly, its SCR activity is even promoted by SO_2 at low moisture conditions [20,21]. These behaviors were attributed to AC's high capabilities for NH_3 adsorption especially in the presence of adsorbed SO_2 [21,22] and to its catalytic activities for reactions of NO with NH_4HSO_4, a poison formed in the presence of SO_2 [22]. To validate these suggestions and to further improve activity of V_2O_5/AC, the SCR mechanism should be studied in detail.

Many studies have been made to understand behaviors of the SCR reaction over V_2O_5/AC catalyst, including those employing temperature-programmed desorption (TPD) [19,23], transient response technique and diffuse reflectance infrared Fourier transform spectroscopy (DRIFTS) [24], and different mechanisms were proposed. Adsorption and activation (partial oxidation) of NH_3 were recognized as a key step in all the mechanisms even though detailed information on adsorption and activation of NH_3 was scarce, such as the roles of AC and V_2O_5. While the information for AC and V_2O_5/TiO_2 catalysts is valuable for understanding V_2O_5/AC's behavior in the SCR, such as formation of $CO^-(NH_4)^+$ on the AC surface [25] and strong adsorption of NH_3 on V_2O_5 [26,27], experimental evidence and theoretical analysis on V_2O_5/AC are still crucial. This paper carries out such a research using TG, MS and DRIFTS techniques.

2. Experimental

2.1. Preparation of V_2O_5/AC

A commercial activated coke (AC) with sizes of 30–60 meshes was impregnated using the incipient wetness method with an aqueous solution containing NH_4VO_3 and oxalic acid. The sample

* Corresponding author at: State Key Laboratory of Coal Conversion, Institute of Coal Chemistry, Chinese Academy of Sciences, Taiyuan 030001, PR China.
Tel.: +86 351 4053091; fax: +86 351 4053091.
E-mail address: zyliu@sxicc.ac.cn (Z. Liu).

0926-3373/$ – see front matter © 2009 Elsevier B.V. All rights reserved.
doi:10.1016/j.apcatb.2009.09.005

was then dried at 50 °C for 6 h and at 110 °C for 12 h, calcined in N_2 at 500 °C for 5 h, and preoxidized in air at 250 °C for 5 h. By adjusting NH_4VO_3 concentration in the solution, V_2O_5/AC catalysts containing 1, 2 and 5 wt% V_2O_5 were prepared and termed 1%V_2O_5/AC, 2%V_2O_5/AC and 5%V_2O_5/AC, respectively.

2.2. Characterization of the catalysts

TPD experiment was carried out in a fixed bed reactor of 10 mm in inner diameter. A catalyst sample of 0.150 g was loaded into the reactor, dried at 120 °C for 0.5 h and then cooled to 30 °C in a flow of Ar. The Ar flow was then replaced by a flow containing 1500 ppm NH_3/Ar at a rate of 100 ml/min for 1 h for NH_3 adsorption. This was then followed by an Ar purge for 0.5 h and TPD from 30 to 500 °C at a heating rate of 10 °C/min. The effluent was monitored on-line by a mass-quadrupole (MS) detector (OmniStar 200, Blazers).

NH_3 adsorption experiments were carried out in a thermogravimetric (TG) apparatus (TGA 92, Setaram) and a DRIFTS unit. A catalyst sample of 0.030 g was pretreated in the TG at 120 °C for 0.5 h to remove H_2O. After cooling down the sample to 30 °C, a flow of 1500 ppm NH_3/Ar at 100 ml/min was introduced into the TG for NH_3 adsorption for 1 h. The sample was then purged in Ar to a steady state (DTG = 0).

DRIFTS spectra were collected on a Bruker Equinox 55 FTIR instrument with KBr optics and a MCT detector. The diffuse reflectance cell has a controlled environment chamber (0030-102, Spectra-Tech) equipped with ZnSe windows. The spectra were obtained at a resolution of 8 cm^{-1} with 200 scans and collected in Kubelka–Munck mode (a theory of reflectance) without any manipulation. The gaseous streams used in the experiments include 1500 ppm NH_3/Ar, 1500 ppm NO/Ar and 5% O_2/Ar at a total flow rate of 100 ml/min.

3. Results and discussion

3.1. Adsorption of NH_3

3.1.1. The role of V_2O_5 in NH_3 adsorption over V_2O_5/AC

Fig. 1 shows TG curves of NH_3 adsorption on the AC and 1%V_2O_5/AC. To avoid possible NH_3 oxidation, the experiments were carried out at 30 °C. Clearly, V_2O_5 promotes NH_3 adsorption and provides the main adsorption sites, which agrees with that reported for other catalysts [28–32]. The amounts of NH_3 adsorbed at steady state are about 0.017 wt% for AC and 0.302 wt% for 1%V_2O_5/AC. The molar ratio of the adsorbed NH_3 to V_2O_5 is about 3:1, which suggests that NH_3 adsorption has a close relation with V=O bond since there are 4 V=O bonds and 2 V–O bonds in a V_2O_5 molecule.

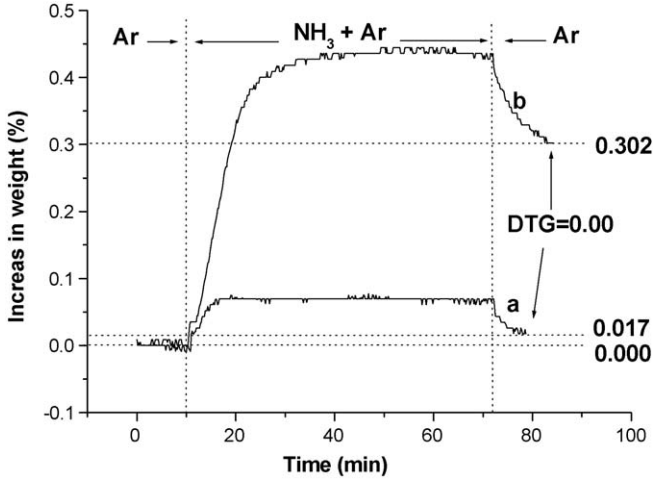

Fig. 1. TG curves of AC (a) and 1%V_2O_5/AC (b) during NH_3 adsorption at 30 °C.

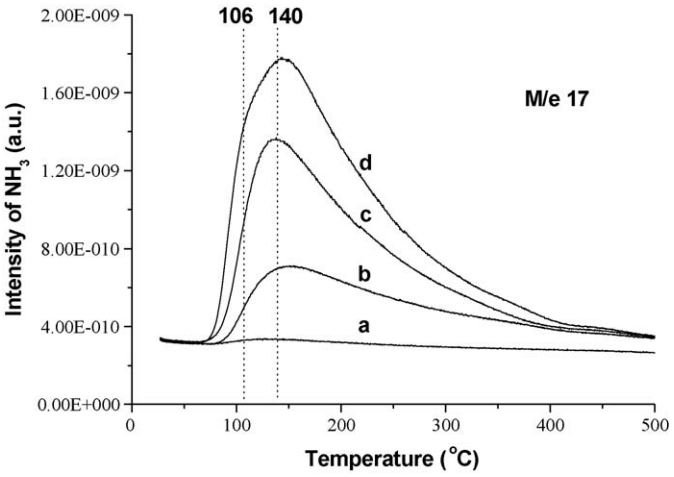

Fig. 2. TPD-MS (NH_3) curves of AC (a), 1%V_2O_5/AC (b), 2%V_2O_5/AC (c) and 5%V_2O_5/AC (d) after NH_3 adsorption at 30 °C.

Fig. 2 shows NH_3 release curves obtained from TPD of the NH_3 adsorbed AC and V_2O_5/AC catalysts. The amount of NH_3 released increases with an increase in V_2O_5 loading, further suggesting that V_2O_5 is the main component to adsorb NH_3. It is interesting to note that the MS curve of 5%V_2O_5/AC (d) shows a shoulder at about 106 °C before the main peak at 140 °C, indicating presence of two types of NH_3 adsorption sites at a high V_2O_5 loading.

3.1.2. NH_3 adsorption over V_2O_5

To better understand the role of V_2O_5 in NH_3 adsorption over V_2O_5/AC, NH_3 adsorption over pure V_2O_5 was studied. Fig. 3 shows a series of DRIFTS spectra of NH_3 adsorbed on a V_2O_5 sample (Analytical grade, Shanghai Kejin Fine Chemicals) at various temperatures. DRIFTS spectra of the V_2O_5 at the same temperatures before the NH_3 adsorption had been subtracted out to facilitate band identification. After exposing the V_2O_5 to NH_3 at 30 °C, several bands appear, including coordinated NH_3 on Lewis acid sites: 3330 (ν_{as}N–H), 3251 (ν_sN–H), 2969 ($2\delta_{as}$H–N–H), 1625 (δ_{as}H–N–H) and 1254 cm^{-1} (δvH–N–H), and NH_4^+ on Brønsted acid sites: 3162 (ν_{as}N–H), 3048 (ν_sN–H), 2801 ($2\delta_{as}$H–N–H), 1687 (δ_{as}H–N–H) and 1448 cm^{-1} (δ_sH–N–H) [4,26,29,30]. Compared with the coordinated NH_3 bands the stronger NH_4^+ bands suggest

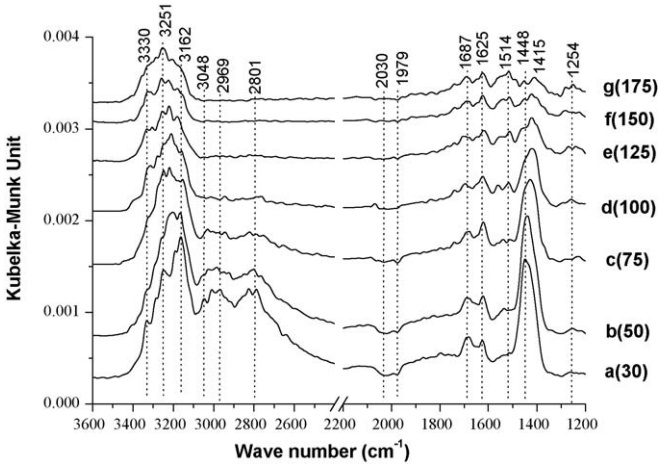

Fig. 3. In situ DRIFTS spectra of V_2O_5 adsorbed with NH_3 at 30 °C (a), 50 °C (b), 75 °C (c), 100 °C (d), 125 °C (e), 150 °C (f) and 175 °C (g).

dominance of NH_4^+ on the V_2O_5 surface. It is important to note that two negative bands at 2030 and 1979 cm^{-1} assigned to V_5^+=O [29–32] are visible, indicating its consumption due to NH_3 adsorption.

Fig. 3 shows that both the NH_4^+ and the coordinated NH_3 bands become weaker at a higher temperature, but the decreases in NH_4^+ bands are more significant than that in coordinated NH_3 bands, suggesting that the coordinated NH_3 is thermally more stable than NH_4^+. At 175 °C, the strong NH_4^+ band at 1448 cm^{-1} shifts to 1415 cm^{-1} and becomes smaller than that of the coordinated NH_3, and a band at 1514 cm^{-1} assigned to NH_2 appears. This indicates that the V_2O_5 has an ability to oxidize (or dehydrogenize) NH_3 into NH_2, which had been considered to be an intermediate of the SCR [3,33–35]. The negative bands at 2030 and 1979 cm^{-1} gradually disappear at higher temperatures, indicating recovery of V=O sites due to reduced NH_3 adsorption on the V_2O_5 surface.

3.1.3. Adsorption of NH_3 over V_2O_5, AC and V_2O_5/AC at 200 °C

Fig. 4 shows DRIFTS spectra of different samples exposed to NH_3 at 200 °C for 1 h and then purged with Ar. DRIFTS spectra of these samples before the NH_3 adsorption had been subtracted out for better band identification. The spectrum of V_2O_5 (Fig. 4a) shows NH_2 (1514 cm^{-1}), imide (1585 and 1342 cm^{-1}) [3,36], V=O (2030 and 1979 cm^{-1}, negative) and NO (1864 cm^{-1}, weak) [37] besides NH (3000–3400 cm^{-1}) and NH_3 (1625 cm^{-1}), indicating oxidation of the adsorbed NH_3 over V_2O_5 at 200 °C. Since there was no O_2 in the gas phase, the oxidation of NH_3 can only be attributed to consumption of V=O on the V_2O_5 surface, suggesting V=O being the main sites for NH_3 adsorption and oxidation.

The spectrum of NH_3 adsorbed on AC (Fig. 4b) also shows the presence of NH, NH_3, and NH_2. The shoulder band at 1559 cm^{-1} and the weak band at 1700 cm^{-1} indicate the presence of acylamide [33,38] due to interaction of NH_3 with the oxygen-containing functional groups on the AC surface. These indicate that, at 200 °C, NH_3 can be adsorbed on the AC's Lewis acid sites and oxidized to form NH_2 and an acylamide structure.

Compared with AC (Fig. 4b), 1%V_2O_5/AC (Fig. 4c) shows increased NH (a stronger band at 3231 cm^{-1}), NH_3 (a new band at 2969 cm^{-1} and a stronger band at 1625 cm^{-1}), NH_2 (1514 cm^{-1}) and acylamide (1700 cm^{-1}), suggesting increased NH_3 adsorption and oxidation due to V_2O_5.

Compared with AC and 1%V_2O_5/AC, 2%V_2O_5/AC (Fig. 4d) shows stronger and more complicated NH bands and increased NH_2 and acylamide bands, suggesting a higher oxidation activity. The increased bands of NH_3 on Lewis acid sites and NH_4^+ on Brϕnsted acid sites may be attributed to oxidation of the AC surface by V_2O_5 or by the pre-oxidation step used in preparation of V_2O_5/AC, which promotes NH_3 adsorption and forms ammonium salts of carboxylic acids [33].

The DRIFTS spectra in Fig. 4 indicate that V=O in V_2O_5/AC is mainly responsible for the high activities of NH_3 adsorption and oxidation, although direct information on V=O is limited due possibly to the strong IR adsorption of AC that covers up the weak adsorption of V=O.

3.2. Oxidation of NH_3

3.2.1. Oxidation of NH_3 over V_2O_5 and AC

Fig. 5 shows DRIFTS spectra of V_2O_5 at various temperatures during TPD (A) and TPO (B) following NH_3 adsorption at 30 °C. These spectra were obtained by subtracting the raw spectra by that of V_2O_5 itself under the same conditions. As discussed earlier, the NH_3 adsorption yields bands of coordinated NH_3 on Lewis acid sites, NH_4^+ on Brϕnsted acid sites, and negative peaks of V=O. The differences in changes in IR bands during the two heating processes are observable. In TPD an increase in temperature results in decreases in IR bands of NH_3, NH_4^+ and V=O (negative), suggesting depletion of surface N-containing species and recovery of V=O structure. In TPO, however, these decreases are faster, as evidenced by the smaller bands of NH_3 (1621 cm^{-1}) and NH_4^+ (1435 cm^{-1}) at 125 °C and the fewer bands (3256 cm^{-1}) at 200 °C compared with that in TPD, indicating increased oxidation in the presence of O_2.

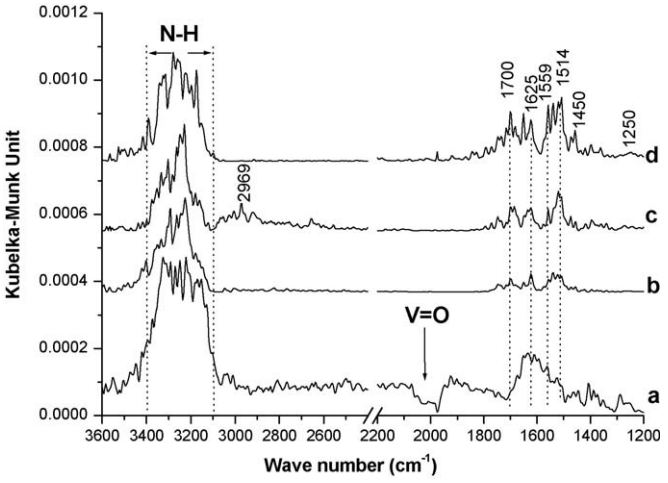

Fig. 4. In situ DRIFTS spectra of V_2O_5 (a), AC (b), 1%V_2O_5/AC (c) and 2%V_2O_5/AC (d) adsorbed with NH_3 at 200 °C.

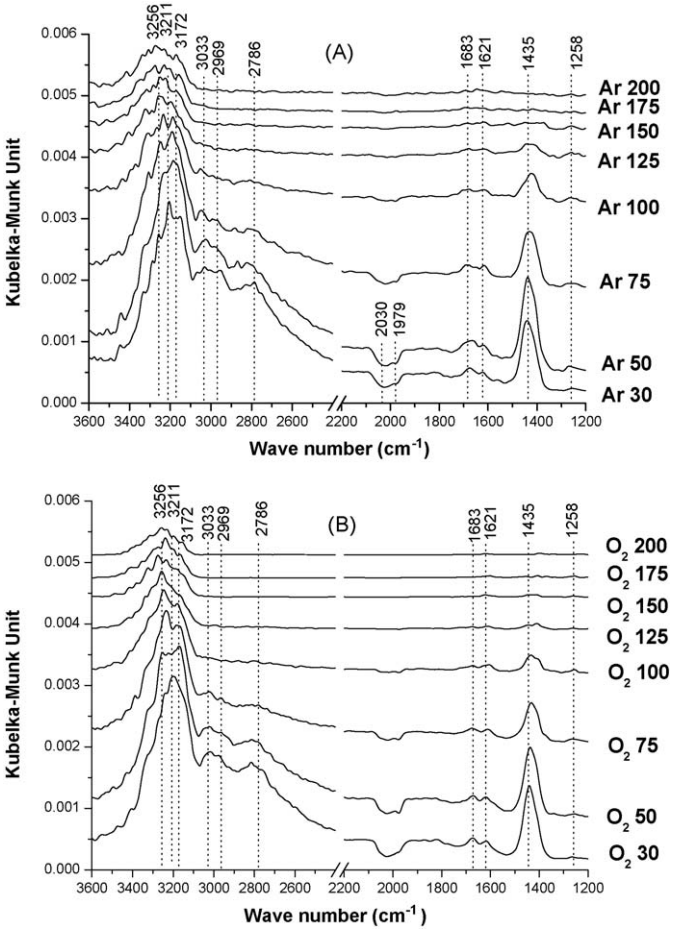

Fig. 5. In situ DRIFTS spectra of V_2O_5 at various temperatures (°C) during TPD in Ar (A) and TPO in 5%O_2/Ar (B) after NH_3 adsorption at 30 °C for 1 h.

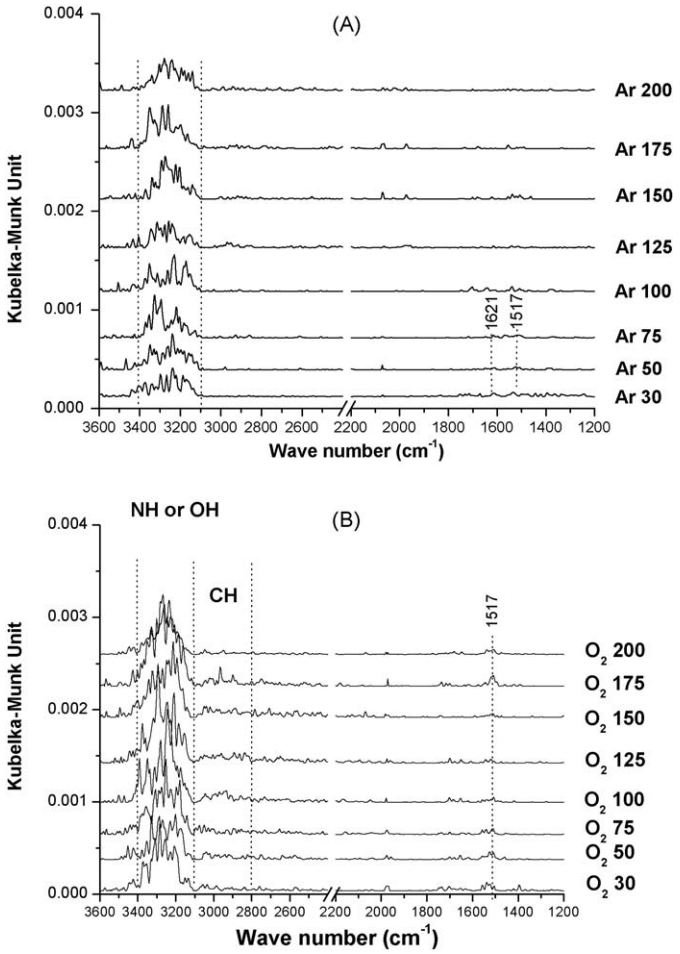

Fig. 6. In situ DRIFTS spectra of AC at various temperatures (°C) during TPD in Ar (A) and TPO in 5%O_2/Ar (B) after NH_3 adsorption at 30 °C for 1 h.

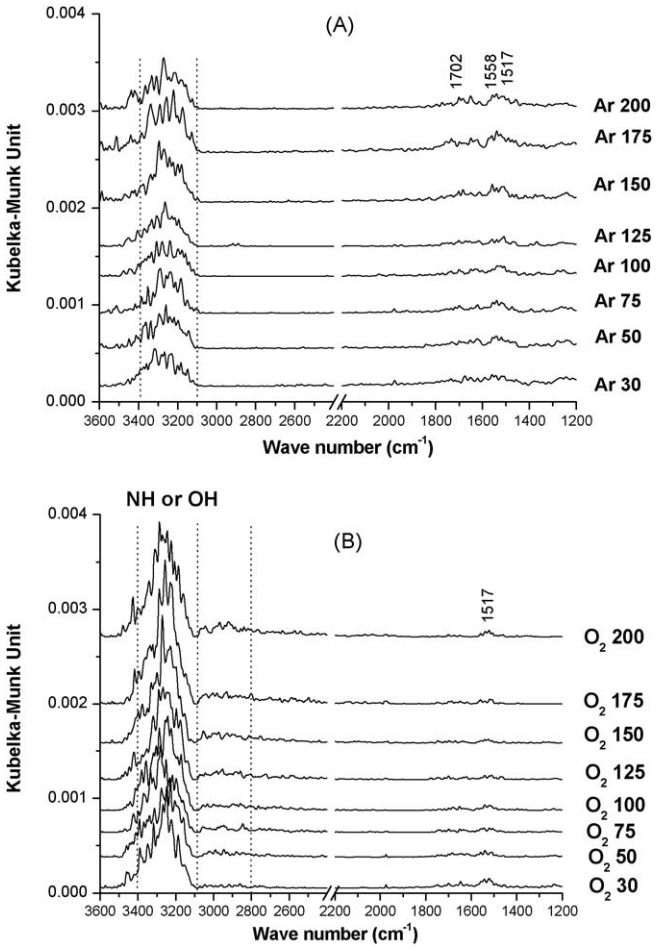

Fig. 7. In situ DRIFTS spectra of 2%V_2O_5/AC at various temperatures (°C) during TPD in Ar (A) and TPO in 5%O_2/Ar (B) after NH_3 adsorption at 30 °C for 1 h.

The relative changes in bands of coordinated NH_3 (3256 cm^{-1}) and NH_4^+ (3172 cm^{-1}) with the increasing temperature are also different. In TPD, at 30 °C, the band of NH_4^+ is much stronger than that of NH_3, indicating dominance of NH_4^+ on the surface. With an increase in temperature the band of NH_3 becomes relatively stronger than that of NH_4^+, as evidenced by their similar intensity at 100 °C and a higher intensity of NH_3 than that of NH_4^+ at 200 °C. This trend occurs also in TPO, but at temperatures lower than that in TPD. Clearly, the NH_4^+ on Brϕnsted acid sites is thermally less stable and easier to be oxidized than the coordinated NH_3 on Lewis acid sites.

Fig. 6 shows DRIFTS spectra of AC at various temperatures during TPD (A) and TPO (B) following NH_3 adsorption at 30 °C. Again, these spectra were obtained by subtracting the raw spectra by that of the AC itself under the same conditions. Fig. 6A shows weak NH_3 adsorption on the AC as indicated by the only obvious NH vibration bands at 3100–3400 cm^{-1}. The disappearance of the weak bands at 1621 and 1517 cm^{-1} with increasing temperature indicates intricate structure of NH on the AC surface corresponding to changes in bands at 3100–3400 cm^{-1}.

Compared with Fig. 6A, Fig. 6B shows stronger NH bands, new CH bands (2800–3100 cm^{-1}) as well as a weak NH_2 band (near 1517 cm^{-1}) [3,37,39] indicating oxidation of NH_3 by O_2 on the AC surface.

3.2.2. Oxidation of NH_3 over V_2O_5/AC

Fig. 7 shows DRIFTS spectra of 2%V_2O_5/AC at various temperatures during TPD (A) and TPO (B) following NH_3 adsorption at 30 °C. The same as before, these spectra were obtained by subtracting the raw spectra by that of 2%V_2O_5/AC itself under the same conditions. Comparing with that of AC in Fig. 6A, Fig. 7A shows stronger NH_3 bands. The appearance of the bands at 1558 and 1702 cm^{-1} and the increase in band at 1517 cm^{-1} indicate oxidation (or dehydrogenation) of NH_3 into NH_2 and acylamide species by V_2O_5 in the absence of O_2.

Similar to Fig. 6, Fig. 7B shows stronger NH and CH bands than Fig. 7A, suggesting increased NH_3 adsorption by O_2. The smaller bands at 1702, 1558 and 1517 cm^{-1} than those in Fig. 7A, especially at high temperatures, mean consumption of NH_2 and acylamide structures through reactions with O_2. The acylamide structures seem more active than NH_2 because their bands disappear at faster rates.

Acylamide structure and NH_2 had been proposed to be intermediates of the SCR. Their formation on V_2O_5/AC and disappearance in O_2 do not suggest a negative role of O_2 in activation of adsorbed NH_3, because the reduced active sites on V_2O_5/AC by NH_3 activation (partial oxidation) need to be restored by gaseous O_2.

To further understand the role of O_2, 2%V_2O_5/AC was pretreated in Ar or in 5%O_2/Ar at 200 °C for 0.5 h before NH_3 adsorption at 30 °C. The sample pretreated in Ar (Fig. 8A) shows bands of NH_3 on Lewis acid sites, NH_4^+ on Brϕnsted acid sites, and amine (near 1560 and 1698 cm^{-1} [30,36]). In comparison, the sample pretreated in 5%O_2/Ar (Fig. 8B) shows a higher NH_4^+ band, suggesting reactions of NH_3 with carboxylic structure formed on the AC surface in the O_2 treatment, and a stronger NH_2 band at 1519 cm^{-1}, indicating

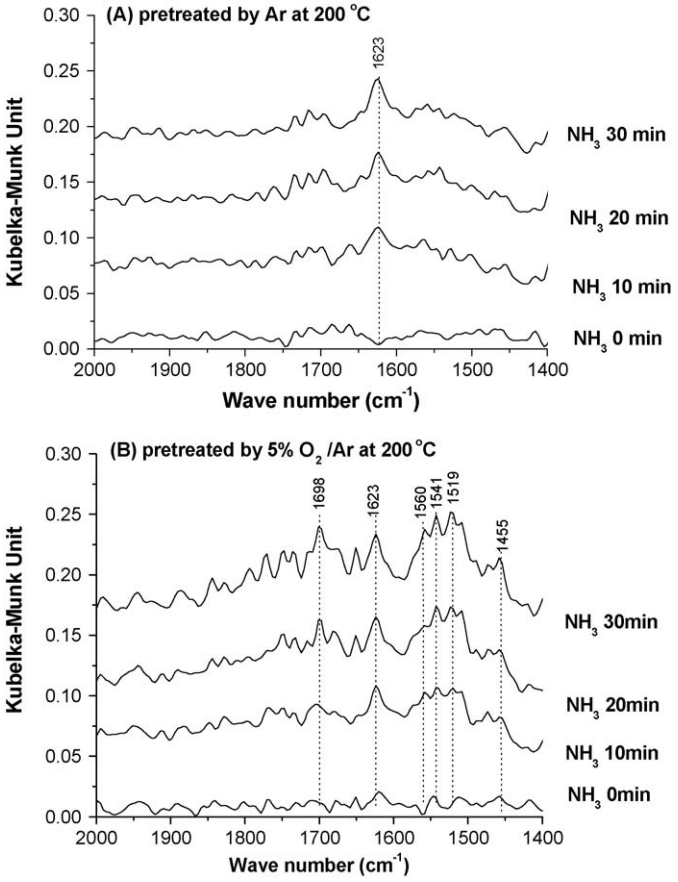

Fig. 8. In situ DRIFTS spectrum of V_2O_5/AC pretreated by Ar (A) or 5%O_2/Ar (B) at 200 °C and then adsorbed with NH_3 at 30 °C for 0 min (a), 10 min (b), 20 min (c) and 30 min (d).

partial oxidation (or dehydrogenation) of the adsorbed NH_3. The two strong bands near 1698 and 1560–1541 cm^{-1}, assigned to interactions between NH_3 and C═O and termed amide bands I and II in the literature [33,40], indicate formation of C═O group in the O_2 treatment. Clearly, the O_2 treatment not only results in more NH_4^+ on Brϕnsted acid sites on the V_2O_5/AC surface but also a higher oxidation activity.

3.2.3. Oxidation of NH_3 by O_2

Due to progressive oxidation with increasing temperature, behavior of NH_3 oxidation at 200 °C is not clearly seen in Fig. 7B. Therefore, 2%V_2O_5/AC was subjected to co-adsorption of NH_3 and O_2 at 200 °C followed by Ar purging and exposure to a mixture of NO and O_2. The DRIFTS spectra of the experiment are shown in Fig. 9. After the 30 min co-adsorption, the catalyst shows obvious bands at 2217 and 1083 cm^{-1}, indicating formation of isocyanate species (NCO) [33] and CN bond in a $C(NH_2)$ structure, respectively. These species seem quite stable since they change little during the Ar purging. It should be noted that the changes in NCO and $C(NH_x)$ may be interrelated, $C(NH_2)$ may be oxidized by O_2 to form NCO which is an intermediate for the formation of N_2 or NO.

Introduction of NO and O_2 reduces the $C(NH_2)$ band due to its participation in the SCR reaction and eliminates the NCO band due to oxidation with O_2. The formation of new bands at 2194 and 2178 cm^{-1} may result from split of the band at 2180 cm^{-1} assigned to N≡N vibration in N_2^- ions [3], indicating formation of N_2 through continued oxidation of C–NH_2 to NCO. Those mean that gaseous O_2 plays an important role in oxidation of NH_3 to N_2.

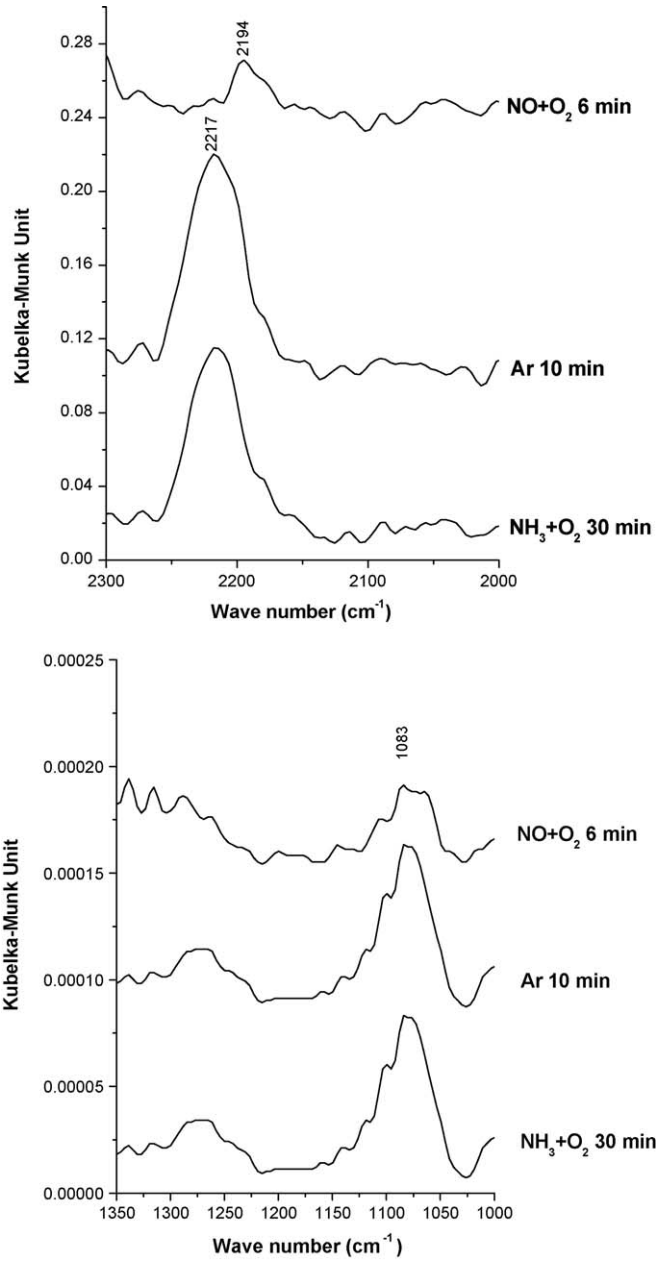

Fig. 9. In situ DRIFTS spectrum of 2%V_2O_5/AC subjected to NH_3 adsorption in the presence of O_2 at 200 °C and then exposure to a mixture of NO and O_2.

4. Conclusions

V_2O_5/AC has higher abilities for NH_3 adsorption and oxidation than AC due mainly to the presence of V_2O_5. V_2O_5 has Brϕnsted and Lewis acid sites. The NH_4^+ on Brϕnsted acid sites is thermally less stable and easier to be oxidized than the coordinated NH_3 on Lewis acid sites. V═O bond is the main sites for the role of V_2O_5. In addition to NH_4^+ on Brϕnsted acid sites and NH_3 on Lewis acid sites, NH_3 adsorption on V_2O_5/AC at 200 °C yields also NH_2 and acylamide, the latter is more active than the former in the presence of O_2.

Gaseous O_2 promotes adsorption and oxidation of NH_3 over V_2O_5/AC to form more NH_4^+, NH_2 and acylamide species. It also promotes the reaction of NH_3 with C to form a $C(NH_2)$ structure, which is active for SCR or is further oxidized into N_2 via an intermediate isocyanate species NCO.

Acknowledgements

The authors gratefully acknowledge the financial support from the Natural Science Foundation of China (20877078, 20736001 and 20821004) and the National High Technology Research and Development Program of China (2007AA05Z310).

References

[1] P. Balle, B. Gelger, S. Kuretl, Appl. Catal. B 85 (2009) 109.
[2] S. Yamazoe, Y. Masutani, K. Teramura, Y. Hitomi, T. Shishido, T. Tanaka, Appl. Catal. B 83 (2009) 123.
[3] G. Ramis, L. Yi, G. Busca, M. Turco, E. Kotur, R.J. Willey, J. Catal. 157 (1995) 523.
[4] V.I. Parvulescu, S. Boghosiam, V. Parvulescu, S.M. Jung, P. Grange, J. Catal. 217 (2003) 172.
[5] P. Forzatti, Catal. Today 62 (2000) 51.
[6] G. Qi, R.T. Yang, J. Catal. 217 (2003) 434.
[7] J. Zawadzki, M. Wisniewski, Catal. Today 119 (2007) 213.
[8] I. Mochida, Y. Korai, M. Shirahama, S. Kawano, T. Hada, Y. Seo, M. Yoshikawa, A. Yasutake, Carbon 38 (2000) 227.
[9] J. Muniz, G. Marban, A.B. Fuertes, Appl. Catal. B 27 (2000) 27.
[10] Y. Hou, Z. Huang, S. Guo, Catal. Commun. 10 (2009) 1538.
[11] G. Marban, T. V-Solis, A.B. Fuertes, J. Catal. 226 (2004) 138.
[12] J. Pasel, P. Kaßner, B. Montanari, M. Gazzano, A. Vaccari, W. Makowski, T. Lojewski, R. Dziembaj, H. Papp, Appl. Catal. B 18 (1998) 199.
[13] M. Ouzzine, G.A. Cifredo, J.M. Gatica, S. Harti, Appl. Catal. A 342 (2008) 150.
[14] Z. Zhu, Z. Liu, S. Liu, H. Niu, Appl. Catal. B 26 (2001) 25.
[15] Y. Xiao, Q. Liu, Z. Liu, Z. Huang, Y. Guo, J. Yang, Appl. Catal. B 82 (2008) 114.
[16] A. Boyano, M.J. Lazaro, C. Cristiani, F.J. M-Hodar, P. Forzatti, R. Moliner, Chem. Eng. J. 149 (2009) 173.
[17] M.J. Lazaro, M.E. Galvez, C. Ruiz, R. Juan, R. Moliner, Appl. Catal. B 68 (2006) 130.
[18] A. Boyano, N. Lombardo, M.E. Galvez, M.J. Lazaro, R. Moliner, Chem. Eng. J. 144 (2008) 343.
[19] B. Huang, R. Huang, D. Jin, D. Ye, Catal. Today 126 (2007) 279.
[20] Z. Zhu, Z. Liu, H. Niu, S. Liu, J. Catal. 187 (1999) 245.
[21] Z. Zhu, Z. Liu, S. Liu, H. Niu, Appl. Catal. B 30 (2001) 267.
[22] Z. Zhu, H. Niu, Z. Liu, S. Liu, J. Catal. 195 (2000) 268.
[23] T.V. Solis, G. Marban, A.B. Fuertes, Appl. Catal. B 46 (2003) 261.
[24] M.E. Galvez, A. Boyano, M.J. Lazaro, R. Moliner, Chem. Eng. J. 144 (2008) 10.
[25] H. Teng, Y.T. Tu, Y.C. Lai, C.C. Lin, Carbon 39 (2001) 575.
[26] M.A. Centeno, I. Carrizosa, J.A. Odoriozola, Appl. Catal. B 29 (2001) 307.
[27] N.Y. Topsøe, H. Topsøe, J.A. Dumesic, J. Catal. 151 (1995) 241.
[28] Q. Liu, Z. Liu, C. Li, Chin. J. Catal. 27 (2006) 636.
[29] M.A. Centeno, I. Carrizosa, J.A. Odoriozola, Phys. Chem. Chem. Phys. 1 (1999) 349.
[30] S.M. Jung, P. Grange, Appl. Catal. B 36 (2002) 325.
[31] C.-H. Lin, H. Bai, Ind. Eng. Chem. Res. 43 (2004) 5983.
[32] L. Lietti, P. Forzatti, G. Ramis, G. Busca, F. Bregani, Appl. Catal. B 3 (1993) 13.
[33] J. Zawadzki, M. Wisniewski, Carbon 41 (2003) 2257.
[34] L. Lietti, J. Svachula, P. Forzatti, G. Busca, G. Ramis, F. Bregani, Catal. Today 17 (1993) 131.
[35] M. Armandi, B. Bonelli, Appl. Catal. B 70 (2007) 585.
[36] G. Qi, R.T. Yang, J. Phys. Chem. 108 (2004) 15738.
[37] G. Ramis, G. Busca, F. Bregani, P. Forzatti, Appl. Catal. B 64 (1990), 259. B.
[38] D.J. Skrovanek, S.E. Howe, P.C. Painter, M.M. Coleman, Macromolecules 18 (1985) 1676.
[39] G. Xie, Z. Liu, Z. Zhu, Q. Liu, J. Ge, Z. Huang, J. Catal. 224 (2004) 42.
[40] M.A. Larrubia, G. Ramis, G. Busca, Appl. Catal. B 27 (2000) L145.